Article

Cell Reports

Impact of Dietary Interventions on Noncoding RNA Networks and mRNAs Encoding Chromatin-Related Factors

Graphical Abstract

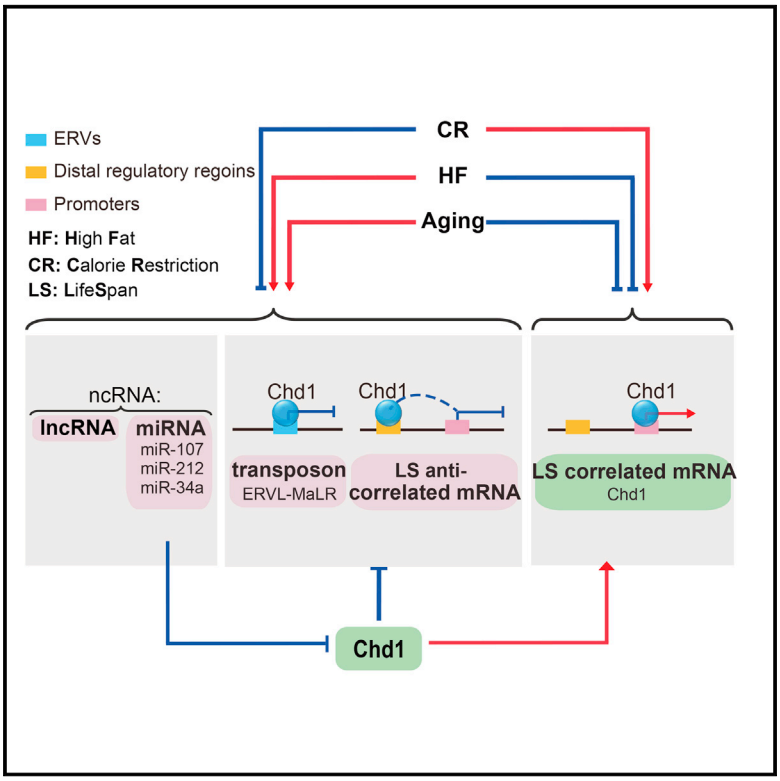

Authors

Christopher D. Green, Yi Huang, Xiaoyang Dou, Liu Yang, Yong Liu, Jing-Dong J. Han

Correspondence

jdhan@picb.ac.cn

In Brief

Through liver RNA sequencing and microRNA sequencing in mice across multiple energy intake and expenditure interventions, Green et al. found lifespan-extending interventions largely repressed the expression of miRNAs, lncRNAs, and transposable elements; miRNAs preferentially target mRNAs whose expression positively correlated with lifespan and modulate expression by targeting genes with chromatin-related functions.

Highlights

- Dietary interventions dramatically modulate midlife liver ncRNA expression
- mRNAs positively correlated with long lifespan are highly targeted by miRNAs
- Lifespan-related miRNAs preferentially target Chd1 and other chromatin-related genes
- Chd1 knockdown mimics changes induced by a high-fat diet or aging

Accession Numbers

GSE87514

Green et al., 2017, Cell Reports *18*, 2957–2968
March 21, 2017
http://dx.doi.org/10.1016/j.celrep.2017.03.001

Cell Reports
Article

Impact of Dietary Interventions on Noncoding RNA Networks and mRNAs Encoding Chromatin-Related Factors

Christopher D. Green,[1,4] Yi Huang,[1,4] Xiaoyang Dou,[1,2,4] Liu Yang,[3] Yong Liu,[3] and Jing-Dong J. Han[1,5,*]
[1]Key Laboratory of Computational Biology, CAS Center for Excellence in Molecular Cell Science, Collaborative Innovation Center for Genetics and Developmental Biology, Chinese Academy of Sciences-Max Planck Partner Institute for Computational Biology, Shanghai Institutes for Biological Sciences, Chinese Academy of Sciences, 320 Yue Yang Road, Shanghai 200031, China
[2]University of Chinese Academy of Sciences, Beijing 100049, China
[3]Key Laboratory of Nutrition and Metabolism, Institute for Nutritional Sciences, Shanghai Institutes for Biological Sciences, Chinese Academy of Sciences, Shanghai 200031, China
[4]Co-first author
[5]Lead Contact
*Correspondence: jdhan@picb.ac.cn
http://dx.doi.org/10.1016/j.celrep.2017.03.001

SUMMARY

Dietary interventions dramatically affect metabolic disease and lifespan in various aging models. Here, we profiled liver microRNA (miRNA), coding, and long non-coding RNA (lncRNA) expression by high-throughput deep sequencing in mice across multiple energy intake and expenditure interventions. Strikingly, three dietary intervention network design patterns were uncovered: (1) lifespan-extending interventions largely repressed the expression of miRNAs, lncRNAs, and transposable elements; (2) protein-coding mRNAs with expression positively correlated with long lifespan are highly targeted by miRNAs; and (3) miRNA-targeting interactions mainly target chromatin-related functions. We experimentally validated miR-34a, miR-107, and miR-212-3p targeting of the chromatin remodeler *Chd1* and further demonstrate that *Chd1* knockdown mimics high-fat diet and aging-induced gene expression changes and activation of transposons. Our findings demonstrate lifespan-extending diets repress miRNA-chromatin remodeler interactions and safeguard against deregulated transcription induced by aging and lifespan shortening diets, events linked by microRNA, chromatin, and ncRNA crosstalk.

INTRODUCTION

Lifestyle interventions, such as modulating dietary macronutrients, caloric intake, and energy expenditure, can considerably affect the susceptibility to aging-related diseases and, in some cases, an organism's lifespan. Calorie restriction (CR) without malnutrition and other interventions (e.g., voluntary exercise [Ex]) are known to reduce the occurrence of aging-related conditions, including obesity, type II diabetes, and cardiovascular diseases (Mercken et al., 2012). CR, without a compensatory increase in food intake, consistently extends both mean and maximal lifespan in multiple species (Fontana et al., 2010).

Recently, we demonstrated the utility of a multi-intervention approach for identifying genes with lifespan regulatory properties. Mice treated with low-fat (LF) or high-fat (HF) diets plus either voluntary Ex or 30% CR had distinct metabolic and aging-related phenotypes strongly correlated with the extent of lifespan modification by the intervention regimens (Zhou et al., 2012). In a study using the Geometric Framework approach, incremental changes in the ratio of dietary protein, carbohydrate, and fat content led to altered lifespan, which was associated with the activity of mTOR, mitochondrial function, and branched-chain amino acid levels (Solon-Biet et al., 2014). These findings demonstrate the advantage of a multi-intervention approach in uncovering longevity mechanisms that can be missed by single interventions alone. However, little is known about the mechanisms regulating the transcriptional program for longevity across multiple interventions, especially at the epigenetic level.

MicroRNAs (miRNAs) represent a critical class of small, non-coding RNAs (ncRNAs), which regulate a broad range of biological processes. miRNAs contain an approximately 7-nt-long seed region that recognizes and represses target genes either by mRNA degradation or repression of translation (Bartel, 2004). Interestingly, while global profiling found many miRNAs exhibit aging-related expression changes in multiple species and miRNA processing is required for normal lifespan in *C. elegans*, only a few miRNAs in model organisms result in lifespan modifications when modulated, such as *Drosophila* miR-14 and miR-34 and *C. elegans* lin-4, miR-71, miR-124, miR-238, miR-239, and miR-246 (Boehm and Slack, 2005; de Lencastre et al., 2010; Liu et al., 2012; Wang et al., 2014b; Xu et al., 2003). This is likely due to the functional redundancy of miRNAs, as they recognize many, often overlapping, target genes (Kato and Slack, 2013). More recently, dietary-restriction-induced longevity in *C. elegans* was found to be mediated in part by miR-71 and miR-228 or mimicked by deletion of

miR-80 (Smith-Vikos et al., 2014; Vora et al., 2013). In mammals, miRNAs affect various aging-related phenotypes. For example, miR-34a, which can induce cellular apoptosis and senescence, is upregulated in the aging heart and contributes to cardiac dysfunction in old mice (Boon et al., 2013; Christoffersen et al., 2010; He et al., 2007). Global profiling has also identified miRNAs differentially expressed with age and reversed by CR (Khanna et al., 2011; Mercken et al., 2013; Mori et al., 2012; Olivo-Marston et al., 2014). Compared to miRNAs, less is known about nutrient regulation and longevity-related functions of other ncRNA classes.

Here, we investigated midlife liver transcriptome changes in our model of dietary/lifestyle interventions that modify aging-related phenotypes, liver physiology, and mean/maximum lifespan (Zhou et al., 2012). Specifically, we profiled the expression of both mRNAs and ncRNAs, including miRNAs, long ncRNAs (lncRNAs), and transposable elements, by high-throughput deep sequencing. Among all analyzed ncRNAs with expression correlated with mean lifespan, we surprisingly found a significantly larger proportion to have decreased expression with longer lifespan, compared to protein-coding mRNAs. Examination of the miRNA regulatory potential of lifespan-related mRNAs showed that genes with increased expression with long lifespan were much more likely to be targets of miRNAs. Interestingly, both pathway enrichment and bipartite network analyses revealed miRNAs targeting genes with chromatin-related functions, such as the chromatin remodeler *Chd1*. Furthermore, we demonstrate that *Chd1* knockdown mimics HF diet and aging-induced gene expression changes and transposon activation. Together, these findings reveal a dramatic global repression of transposons by lifespan-extending interventions, safeguarding chromatin from leaky transcription and deregulation of gene expression, at least in part, through miRNA-chromatin remodeler interactions.

RESULTS

Midlife Liver Physiology and Transcriptome Analysis during Different Intervention Regimens

To characterize lifespan-related liver transcriptome changes mediated by different intervention regimens, we selected 18 male C57BL/6J mice at 62 weeks of age (midlife) that underwent one of six lifestyle interventions (n = 3), which we previously demonstrated to significantly affect lifespan (Zhou et al., 2012). These interventions included low-fat (LF) diet, high-fat (HF) diet, LF or HF diet with access to voluntary wheel running Ex, and LF or HF diet with CR to 70% of normal food intake. Ordered by the mean lifespan of HF (101 weeks), HF+Ex (114 weeks), LF (127 weeks), LF+Ex (131 weeks), HF+CR (137 weeks), and LF+CR (153 weeks), liver physiological parameters, including liver weight, triglyceride, cholesterol, and the liver damage marker serum aspartate aminotransferase (AST), of the selected samples exhibited an overall reduction with increasing mean lifespan (Figure S1A). This is consistent with the average, which includes two to five extra mice per group that were described previously (Zhou et al., 2012) and, in this study, only used to illustrate the range of the physiological responses to these interventions. Thus, the 18 liver samples utilized in this study display clear functional changes associated with lifespan modification.

By conducting poly(A)+ RNA sequencing (RNA-seq), we detected a total of 12,175 active, annotated transcripts, 11,833 of which are protein coding (Experimental Procedures). Principle component analysis (PCA) shows these lifestyle interventions appear as four distinguishable groups (Figure S1B). According to hierarchical clustering dendrogram, samples are indeed separated into four groups (Figure S1C). LF and HF groups, irrespective of Ex or CR, have noticeably distinct profiles that are further separated by CR. No obvious effect was found for Ex on the global transcription profile, similar to previous findings (Zhou et al., 2012). To identify lifespan-related transcripts, we calculated the Pearson correlation coefficient (PCC) between the mean lifespans and each expressed transcript (log2-transformed) across all 18 samples. We found 1,824 protein-coding transcripts significantly correlated with mean lifespan (PCC $p < 0.01$, an approximate $|PCC| > 0.58$) and distributed nearly equally between negative (913) and positive (911) correlations with lifespan (Figure 1A; Table S1). To validate our RNA-seq data, we compared lifespan PCCs of all transcripts detected both here and in prior microarray data, of which only three sample interventions overlap. This comparison shows a markedly significant correlation between datasets (10,510 transcripts, PCC = 0.62, $p < 2.2e-16$, Figure S1D), and additionally, gene set enrichment analysis (GSEA) of PCC-ranked genes detected by RNA-seq found similar pathways enriched as in the initial study (normalized $p < 0.05$, Table S2, [Zhou et al., 2012]). These results demonstrate that the physiological and transcriptome changes in our intervention model are highly reproducible between different sample sets and analysis platforms.

Unbalanced ncRNA Expression Mediated by Dietary Interventions

We next profiled miRNA expression by small RNA-seq and identified 494 active, annotated miRNAs using SOAP2 (Experimental Procedures). PCA and hierarchical clustering of the miRNA profiles showed comparable separation induced by LF, HF, and CR regimens as for RNA-seq, although the variation was higher for LF and HF+CR groups (Figures S1E and S1F). Analysis of miRNA expression (log2-transformed) found 92 miRNAs significantly correlated with mean lifespan (PCC $p < 0.01$, an approximate $|PCC| > 0.58$). Strikingly, we observed the majority of lifespan-related miRNAs are highly negatively correlated, with 84 negative and eight positive, significantly higher than expected (one-sided binomial test $p = 2.1e-17$, Figure 1B; Table S3). To further confirm the unbalanced distribution of miRNAs in relation to lifespan (LS), in addition to mapping by SOAP2, we also remapped the miRNAs with Burrows-Wheeler Aligner (BWA)/bowtie and used upper quantile/TMM (trimmed mean of M-values) for normalization in addition to reads per million (RPM) as recommended by Tam et al. (2015) (Figure S2A). The conclusions based on different mapping and normalization methods are highly similar. We obtained 13 LS positively correlated and 97 LS negatively correlated miRNAs by the BWA + RPM method, eight LS, positively correlated and 102 LS negatively correlated miRNAs by the BWA + upper quantile method, and nine LS positively correlated and 101 LS negatively correlated by the BWA + TMM method ($p < 0.05$) (Figure S2B). Meanwhile, we calculated PCC of miRNA expression between any

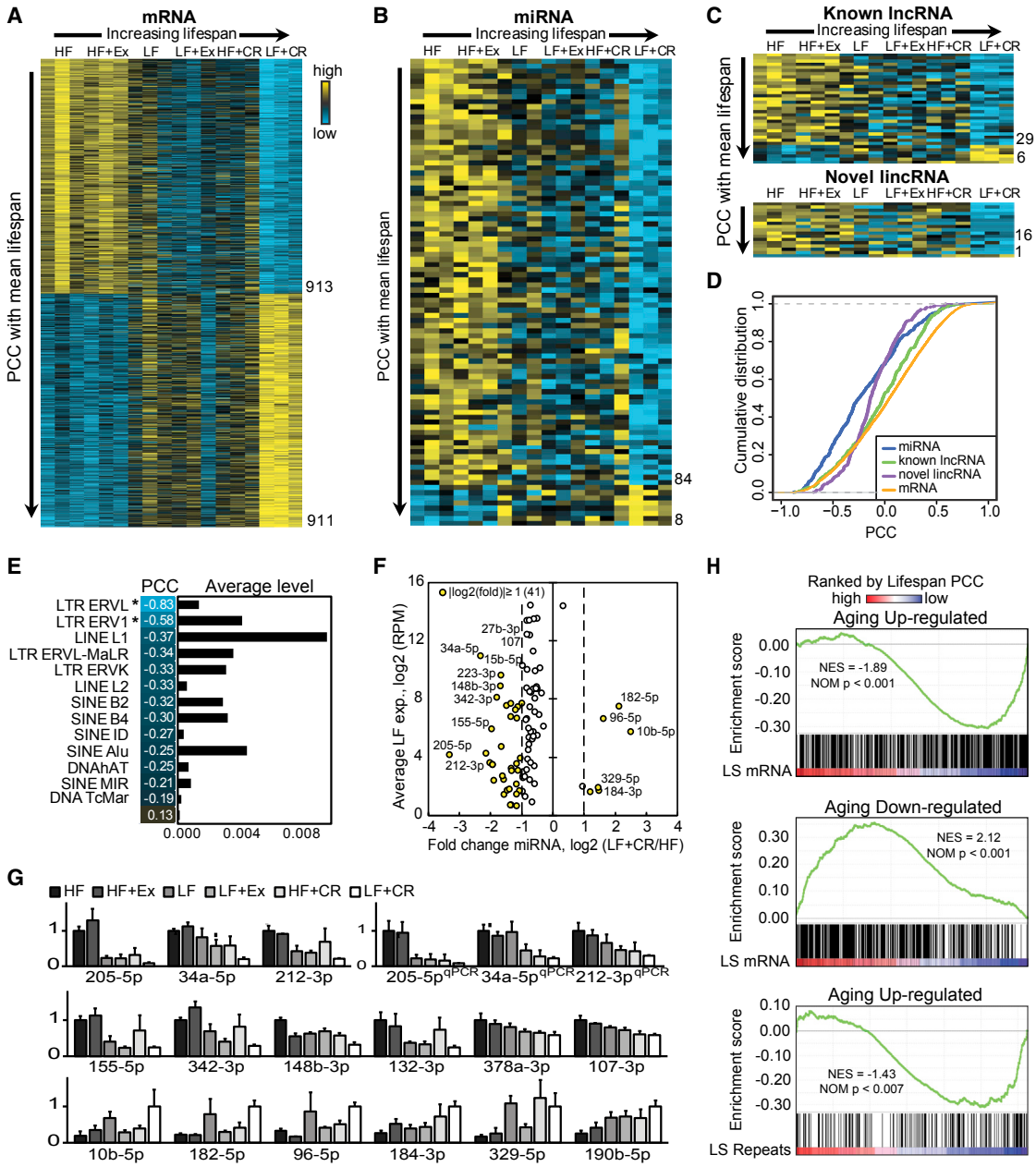

Figure 1. Midlife Liver Transcriptome Responses to Dietary Interventions

(A–C) mRNAs (A), miRNAs (B), and known lncRNAs and novel lincRNAs (C) with expression profiles significantly correlated with mean LS. Data are ranked by increasing Pearson correlation coefficient (PCC) of RNA expression with mean LS. PCC $p < 0.01$.

(D) Cumulative distributions of mean LS PCC values for all detected mRNAs, miRNAs, lncRNAs, and novel lincRNAs.

(E) Average expression levels and PCC values for repeat elements. *$p < 0.01$.

(F) Scatterplot for LS-related miRNA expression (average log2 (RPM) in LF group) versus the log2 fold change in expression for LF+CR relative to HF. Dotted lines separate 41 miRNAs with |log2 fold change| ≥ 1.

(G) Examples of LS-related miRNAs identified by small RNA-seq and validated by qPCR (labeled qPCR and normalized to sno55 RNA). Data represent fold change versus HF (for LS negatively correlated miRNAs) or LF+CR (for LS positively correlated miRNAs) groups. Error bars represent SEM, n = 3.

(H) GSEA analysis for aging-related mRNAs and repeat elements |log2 fold change| ≥ 1.3 enriched in LS-related RNAs (PCC $p < 0.01$). Aging up- and down-regulated genes are differentially expressed genes (DEGs) (t test $p < 0.05$) comparing 21-month with 3-month mice (GEO: GSE57809). LS, lifespan related.

See also Figures S1–S3.

two mapping/normalization methods, and all of them have PCC >0.98 (Figure S2C). Consistently, the miRNA expression correlations with LS are highly correlated between different mapping/normalization methods with PCC >0.93 (Figure S2D).

To determine whether this phenomenon is apparent in other ncRNAs, we examined annotated lncRNAs detected by RNA-seq (342 in total, Experimental Procedures) and also found a strong trend toward a negative correlation, 29 negative versus six positive (one-sided binomial test p = 5.8e-5, Figure 1C; Table S4). Additionally, high-confidence, long intergenic ncRNAs (lincRNAs) predicted from RNA-seq reads (Experimental Procedures) display a negative trend as well (117 total: eight negative versus zero positive, one-sided binomial test p = 0.0039, Figure 1C). DAVID function enrichment analysis of the nearest coding genes of LS-related lncRNAs revealed that the nearest genes of LS negatively correlated lncRNAs are relatively enriched for peroxisome, and the nearest genes of LS positively correlated lncRNAs are enriched for SET domain compared with all annotated lncRNAs (Figure S2E).

A global comparison of all detected mRNAs and ncRNAs shows a clear shift of ncRNAs, particularly for miRNA and lincRNA, in the cumulative distribution toward more negative expression correlations with mean LS (Figure 1D). Expressed repetitive elements are also largely negatively correlated, including transposon long terminal repeats (LTRs) class L endogenous retroviruses (ERVL) and ERV1 with PCC = −0.83 and −0.58 (PCC p = 2e-5 and 0.02), respectively (Figure 1E). Together, we find significantly unbalanced LS-related ncRNA expression at midlife, largely exhibiting a negative correlation with LS.

To assess the potential relevance of miRNAs highly correlated with LS, we compared the average expression in the LF group to the log2 fold change between the longest and shortest LS groups, respectively, LF+CR and HF (Figure 1F; Table S3). Forty-one miRNAs display an absolute log2 fold change ≥ 1. miR-205-5p shows the greatest change with increasing LS, being reduced by 90% in the LF+CR group relative to HF diet, whereas miR-10b-5p has the highest increase of 5.6-fold (Figures 1F and 1G). We found miR-34a-5p is the highest expressed miRNA and has the third largest fold change (80% reduction). While miR-214-3p and miR-669c-5p have roles implicated in the aging liver (Maes et al., 2008), several LS-related miRNAs, including miR-27b-3p, miR-335-5p, miR-378a-3p, miR-103, and miR-107, were shown to be involved in metabolic disease (Carrer et al., 2012; Nakanishi et al., 2009; Trajkovski et al., 2011; Vickers et al., 2013). miR-34a-5p has been associated with aging, as well as obesity (Choi et al., 2013; Li et al., 2011; Liu et al., 2012), and it consistently has the highest expression fold change among miRNAs both negatively correlated with LS and is elevated in livers of two models of obesity (Figure S2F; Trajkovski et al., 2011). Overall, we identified many miRNAs associated with lifestyle intervention-induced LS modification, several of which have known functional physiological implications.

LS-Correlated mRNA and Repeat Element Expression Display Consistent Aging-Associated Changes

We next examined how our intervention-induced transcriptional responses relate to the aging transcriptome by comparing our findings to RNA-seq data from livers of young (3-month-old) and old (21-month-old) mice (Bochkis et al., 2014). GSEA found genes that are significantly up- or downregulated with age showed a marked enrichment in, respectively, mRNAs negatively (normalized enrichment score [NES] = −1.89, normalized [NOM] p < 0.001) or positively (NES = 2.12, NOM p < 0.001) correlated with LS (Figure 1H). Similar to the effects of LS-shortening diets, ncRNAs tended to exhibit increased expression in aged mice (Figures S3A and S3B). Repeat elements upregulated with age were highly enriched in repeats negatively correlated with LS (NES = −1.43, NOM p < 0.007, Figure 1H), whereas those repressed showed no significant enrichment (Figure S3C). Using a recently published mouse liver miRNA-seq dataset (GEO: GSE65771), we observed more age upregulated (>1.5-fold) liver miRNAs (81 miRNAs) than age downregulated (>1.5-fold, 37 miRNAs). With an even stronger asymmetry, nearly three times as many LS negatively correlated miRNAs are age upregulated (14 miRNAs) as age downregulated (three miRNAs) (Figure S3D). Thus, coding genes, repeat elements, and miRNAs regulated by dietary interventions and highly correlated with LS are largely associated with aging.

LS-Correlated Transcripts Are Enriched for miRNA Target Genes

To explore the regulatory potential of miRNAs identified here, we first utilized the TargetScan database (Lewis et al., 2005) to characterize putative miRNA targets. Based on all expressed miRNAs and transcripts, more negative correlations exist between miRNAs and predicted target genes' expressions, compared to background and randomly chosen simulations (Figure 2A). We also found that, across all possible pairs of expressed miRNAs and transcripts, as the average correlation decreases, the fraction of TargetScan predicted miRNA target pairs increases (Figure 2B). Thus, the predominant negative correlations indicate a greater potential for miRNA regulation of predicted target transcripts. We then examined the enrichment of miRNA target gene sets in our 1,824 LS-related mRNAs. Out of 774 miRNA target gene sets, 298 miRNAs' targets are significantly enriched in the 911 mRNAs positively correlated with LS (permutation p < 0.001, fold ratio = 11.2 versus random expectation), while only three for the 913 negative LS correlated mRNAs (permutation p = 0.003, fold ratio = 0.11 versus random expectation, Figure 2C). Narrowing the miRNA target pair criteria, we find that, among expressed miRNAs, as the negative correlations between miRNAs and target mRNAs become more significant, the enrichment in LS positively correlated mRNA targets increases (Figure 2C; Experimental Procedures). Similarly, LS positively correlated mRNAs are more enriched among all miRNA targets with increasingly more significant negative correlation (Figure 2D).

As HF and CR diets are known to, respectively, increase and decrease inflammation, and activation of immune cells increases expression of genes with shorter 3′ UTRs (Sandberg et al., 2008), we examined the 3′ UTR lengths of our LS-related mRNAs. Interestingly, genes positively correlated with LS have longer 3′ UTRs and may explain, in part, the higher likelihood of these genes being targeted by miRNAs (Figure S4A). To investigate whether mRNAs with similar 3′ UTR lengths would show the same miRNA targeting bias, we binned the positively and negatively regulated

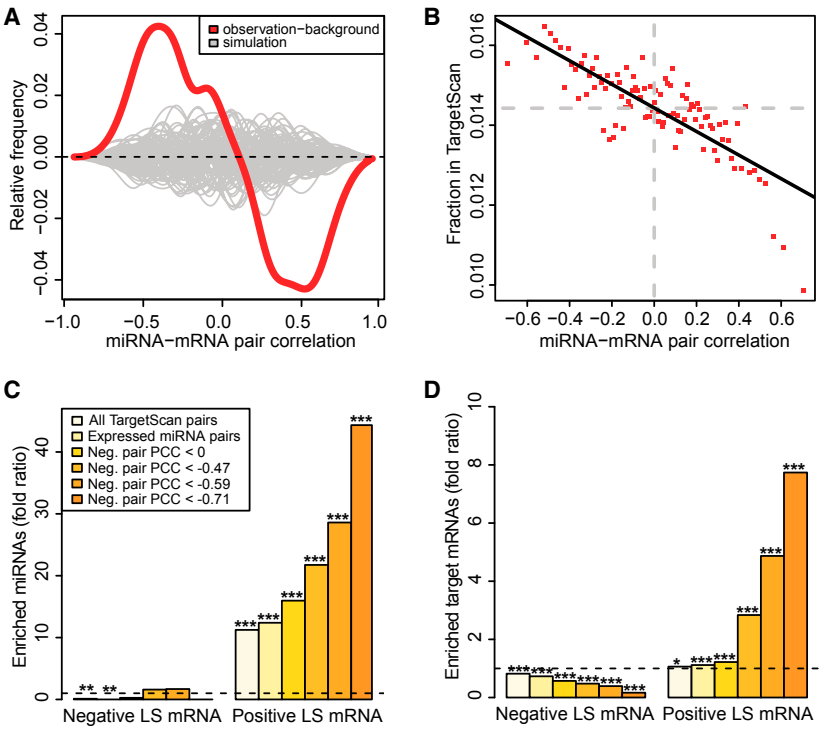

Figure 2. miRNA Regulation of LS-Related mRNAs

(A) miRNA-mRNA target gene pairs exhibit predominantly negative expression correlations. The difference between the relative frequency of miRNA-mRNA target pairs (red line) and background pairs (centered line) at each PCC level was estimated by the R "density" function. Simulated data consisted of randomly selected subsets (permutated 100 times) of the same size from background pairs.

(B) Fraction of all possible miRNA-mRNA pairs in TargetScan database. PCCs of background pairs were equally divided into 100 bins (or levels), each with ~58,455 pairs, and the fraction of TargetScan pairs in each bin were calculated. Vertical dashed line, PCC = 0 or no correlation. Horizontal dashed line, the background fraction. Black line, a linear model of the 100 observations.

(C and D) Enrichment of miRNAs and pooled target genes in the 913 negative or 911 positive LS-related mRNAs under different criteria. In (C), individual miRNAs were regarded as significantly regulating the positively or negatively LS-related mRNA set if one-sided Fisher's exact test $p < 0.05$ for target enrichment. Then significance of the number of these significantly regulating miRNAs was further determined by 1,000 time permutations. The fold ratio was estimated by observation over average background. In (D), all regulating pairs were pooled into one target set. The significance of its overlapping with the LS-related mRNA sets was determined by one-sided Fisher's exact test with Bonferroni correction. The fold ratio was estimated by observation over background expectation.

*$p < 0.05$; **$p < 0.01$; ***$p < 0.001$. LS, lifespan. See also Figure S4.

mRNAs into five ranges according to their 3′ UTR lengths: 0–1,000, 1,000–2,000, 2,000–3,000, 3,000–5,000, and 5,000–maximum bp and then calculated the proportion of mRNAs targeted by miRNAs. When considering miRNAs with predicated targets by TargetScan and expression in liver, we found that, although miRNA targets increase with increased 3′ UTR length for both LS positively and negatively regulated mRNA, LS positively related mRNA are always more likely targeted by LS-related miRNAs than negatively regulated mRNA in all five ranges of 3′ UTR lengths. When considering miRNA with predicated targets by TargetScan and anti-correlated with mRNA (PCC <0), the targeting bias toward LS positively correlated mRNA further increased and the stricter the PCC cutoff was, the more the targeting bias (Figure S4B).

These data suggest that mRNAs induced by CR and associated with long LS are much more likely to be regulated by miRNAs compared to mRNAs that are repressed with long LS.

LS-Related miRNAs Target Genes with Chromatin-Related Functions

Among miRNAs and mRNAs with LS-related expression, 397 miRNA target genes exhibit significant negative miRNA-mRNA pair expression correlations (pair PCC $p < 0.05$, corresponding to PCC < -0.46). Gene ontology (GO) term and Kyoto Encyclopedia of Genes and Genomes (KEGG) pathway enrichment for these 397 target genes indicated functions involved in regulation of transcription, kinase activity, insulin and mTOR pathways, chromatin modification, and histone methyltransferase activity (Figure 3A; Tables S5 and S6). Notably, these targets include 31 aging/LS-related genes curated by the GenAge database (de Magalhães et al., 2005), suggesting that our miRNA targets include many known processes associated with longevity and aging. We then used a network analysis approach to uncover miRNA-target gene interactions. Focusing on miRNA families conserved among vertebrates, we required all miRNA and target gene nodes to have expression profiles significantly related with LS (PCC $p < 0.001$, corresponding to $|PCC| > 0.7$) and the interactions (edges) to have significant negative expression correlations (PCC $p < 0.05$, corresponding to PCC < -0.46, Figure 3B). The reduced network yielded 117 interactions among ten miRNAs and 71 targets. Thirty-three of the interactions have miRNA target pair PCC p values < 0.001, corresponding to PCC < -0.7 (thick edges). In line with the chromatin-related functions, coding gene nodes included chromatin remodelers *Chd1* and *Chd2* and the histone methylation-related genes *Ash1l*, *Epc2*, *Mll1*, and *Mll3*. Interestingly, we identified the strongest negative correlation to exist between miR-34a and *Chd1*, with *Chd1* being targeted by four miRNAs and three of which are highly significantly anti-expressed interactions (PCC $p < 0.001$, corresponding to PCC < -0.7, Figures 3B and 3C). This relatively high degree of significant interactions between *Chd1* and vertebrate conserved miRNAs, together with their seed regions detected in both human and mouse *Chd1*

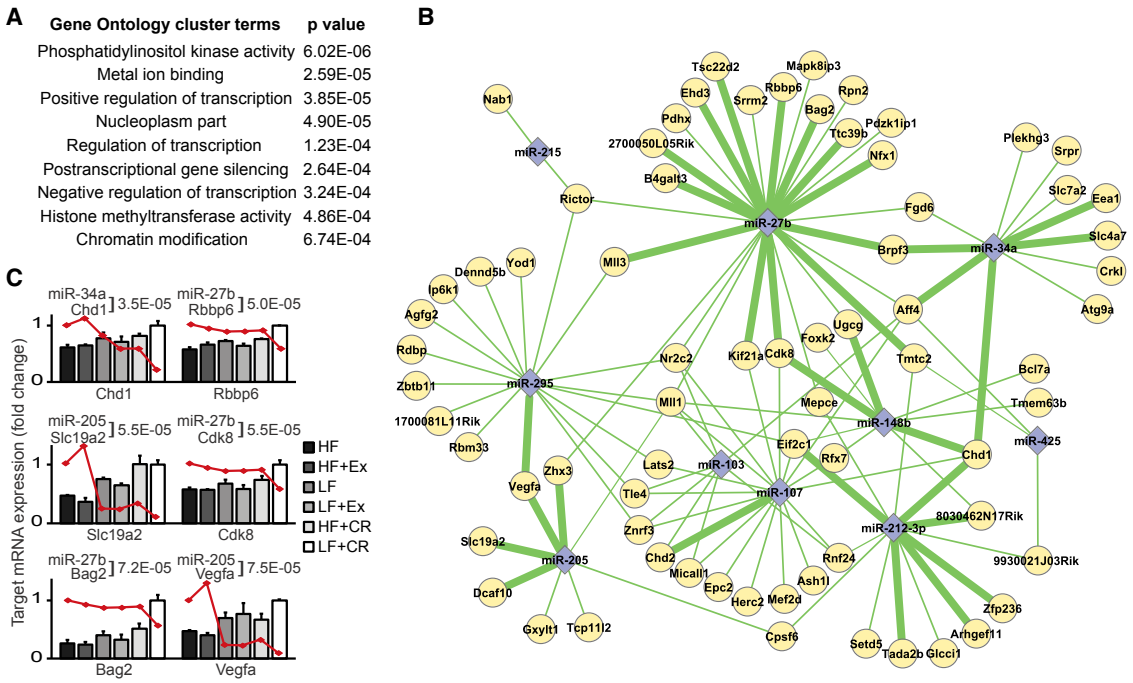

Figure 3. Identification of Pathways and Genes Regulated by LS-Related miRNAs

(A) GO term enrichment for LS-related miRNA target genes (requiring miRNA-mRNA pairs with negative PCC $p < 0.05$). GO clusters include terms with $p \leq 0.001$ and the indicated average term enrichment p value within each cluster.

(B) Network visualization of significantly LS-related miRNA-mRNA target pairs. Nodes represent miRNAs broadly conserved among vertebrates (purple) and target mRNAs (yellow) with expression to mean LS PCC $p < 0.001$. Edges indicate miRNA to mRNA target negative PCCs with $p < 0.05$ to 0.001 (thin line) and < 0.001 (thick line).

(C) Relative expression of mRNAs from top six most significant miRNA-mRNA negative correlations from the network. p values show significance of PCC between indicated miRNA and target gene pairs. Data represent fold change versus LF+CR group. Error bars represent SEM, n = 3. Red line indicates respective miRNA expression fold change versus HF group.

See also Figure S4.

3′ UTRs, indicates these miRNA-*Chd1* interactions are potentially important regulatory events associated with intervention-induced LS modification.

To validate the predicted miRNA-*Chd1* interactions, we measured the ability of a luciferase reporter containing the human *CHD1* 3′ UTR to be targeted by co-transfected mimics for miR-34a, miR-212-3p, miR-107, and miR-148b-3p. Of the four miRNAs, miR-34a, miR-212-3p, and miR-107 significantly repressed the luciferase activity by 20%, 30%, and 40%, respectively (Figure 4A). Subsequent mutation of the miRNA seed regions in the *CHD1* 3′ UTR for miR-34a (one site), miR-212-3p (three sites), and miR-107 (one site) largely blocked the targeting efficiency of each miRNA (Figure 4B). Additionally, all three miRNAs repressed CHD1 at the protein level by ~20%–40% (Figure 4C), further validating the regulation of *CHD1* by these miRNAs. As a control, we also tested the targeting of miR-34a, miR-212-3p, miR-107, and miR-148b-3p to the human *SIRT1* 3′ UTR, a known target of miR-34a. Indeed, miR-34a significantly repressed the luciferase activity by 20%. Unexpectedly, we found the *SIRT1* 3′ UTR was repressed by miR-212-3p, which contains a sequence similar to a known *SIRT1* regulator miR-132-3p (Figures 4D and 4E; Choi and Kemper, 2013). These *Sirt1*-targeting miRNA interactions were not included in the network because *Sirt1* gene expression did not fluctuate across different dietary treatments.

Chd1 Knockdown Mimics High-Fat Diet and Aging-Induced mRNA Expression Changes and Activation of Transposons

Many chromatin regulators not only directly regulate transcription activities, but also guard against insult to the genome and ensure genome stability (Petty and Pillus, 2013). To explore the role of *Chd1* in regulating LS-related genes, we analyzed global expression changes after *Chd1* knockdown (KD) for three published datasets for mouse embryonic stem cells (mESCs) (de Dieuleveult et al., 2016; Gaspar-Maia et al., 2009; Guzman-Ayala et al., 2015) (Supplemental Experimental Procedures). Using GSEA, we found genes upregulated by *Chd1* KD (log2 fold change >1.3, $p < 0.05$) in mESCs were highly enriched for mRNAs negatively correlated with LS, and genes repressed by *Chd1* KD in mESCs were enriched for LS positively correlated mRNAs (Figure 5A). Specifically, genes both upregulated after *Chd1* KD in mESCs (*Chd1* KD in mESCs 2016) and negatively correlated with LS (79 genes) were enriched for GO terms with immune-related functions, and genes both downregulated after *Chd1* KD in mESC and positively correlated with LS (40 genes)

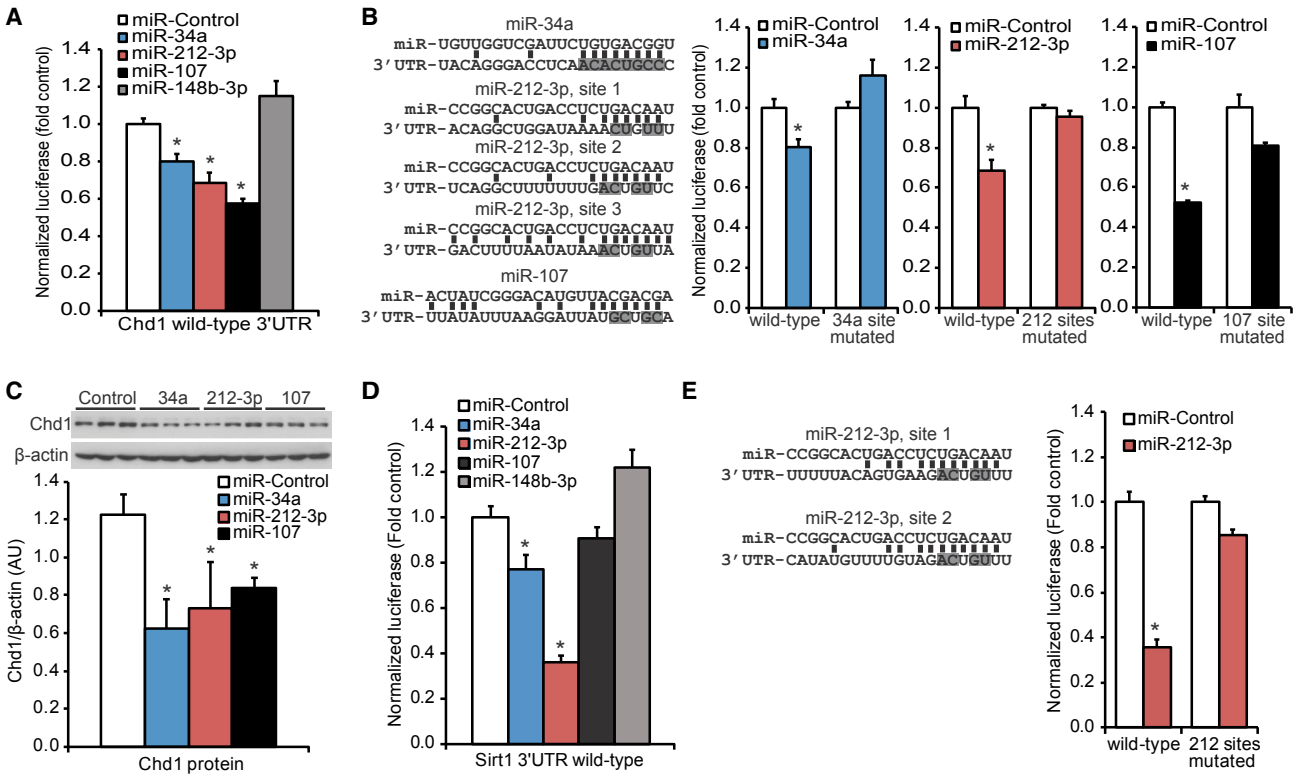

Figure 4. Chromatin Regulators Are Targeted by Multiple LS-Related miRNAs

(A) Luciferase assay for WT *CHD1* 3′ UTR in HeLa cells transfected with miRNA mimics for non-targeting control, miR-34a, miR-212-3p, miR-107, or miR-148b-3p. Error bars depict SD, n ≥ 6. *p < 0.05 versus miR-control.

(B) Left, human miRNA sequences and their corresponding 3′ UTR target sites. Vertical lines indicate complementary bases. Gray highlighted bases mark mutated sites used in subsequent analyses. Right, luciferase assays for *CHD1* 3′ UTR WT or mutated at the indicated sites. Error bars depict SD. *p < 0.05.

(C) Western blot of CHD1 and β-actin from HeLa cells transfected with miRNA mimics for non-targeting control, miR-34a, miR-212-3p, or miR-107. Error bars depict SD, n ≥ 3. *p < 0.03 versus miR-control.

(D) Luciferase assay for WT *SIRT1* 3′ UTR transfected with miRNA mimics for non-targeting control, miR-34a, miR-212-3p, or miR-107. Error bars depict SD, n = 3. *p < 0.05 versus miR-control.

(E) Left, miRNA sequences and their corresponding 3′ UTR target sites. Gray highlighted bases mark mutated sites used in subsequent analyses. Right, luciferase assays for *SIRT1* 3′ UTR WT or mutated at the indicated sites.

Error bars depict SD. *p < 0.05. See also Figure S5.

were enriched for glycolysis/gluconeogenesis functions (Figure 5B). Thus, loss of *Chd1* may contribute to mRNA changes by HF diet and interventions that affect LS.

Chd1 KD-upregulated genes in mESCs tend to negatively correlate with LS, and downregulated genes are positively correlated with LS. To investigate how these two gene sets were simultaneously oppositely regulated by *Chd1*, we analyzed Chd1 chromatin immunoprecipitation sequencing (ChIP-seq) data in mESCs. As expected, *Chd1*-regulated gene and Chd1-targeting gene in mESC show significant overlap (Fisher's exact test p = 4.8E-15), and the overlapping genes are enriched for LS-related genes (Fisher's exact test p = 0.02) (Figure S5A). We separated Chd1 target genes into three categories of genes targeted: only by Chd1 at promoter regions (±2.5 kb upstream and downstream of transcription start site [TSS]), only at enhancer regions (2.5–50 kb away from TSS), and at both enhancer and promoter regions. We found that the first and third categories are significantly LS correlated, whereas the second is significantly LS anti-correlated (GSEA p < 0.001) (Figures 5A, S5B, and S5C). These data suggest that Chd1 may activate LS-correlated genes when binding to their promoters and repress LS anti-correlated genes when binding to their distal regions. The expression activation by Chd1 promoter binding is in line with findings that Chd1 binds H3K4me3 on promoters to promote open chromatin and pluripotency in ESCs (Flanagan et al., 2005; Gaspar-Maia et al., 2009; Sims et al., 2005). The role of *Chd1* in repressing gene expression is, however, consistent with its repression of cryptic transcription (Smolle et al., 2012).

We next examined the role of *Chd1* in activation of transposons and other repetitive elements during aging and by HF. Notably, *Chd1* expression is significantly repressed in old compared to young mice and in KD compared with wild-type (WT) (Figures 5C and S5D). Transposons, such as LTRs ERVL-MaLR and ERVL, largely display elevated expression compared with other repeat elements during aging or HF diet and also have increased expression after *Chd1* KD in mESCs (for aging, t test

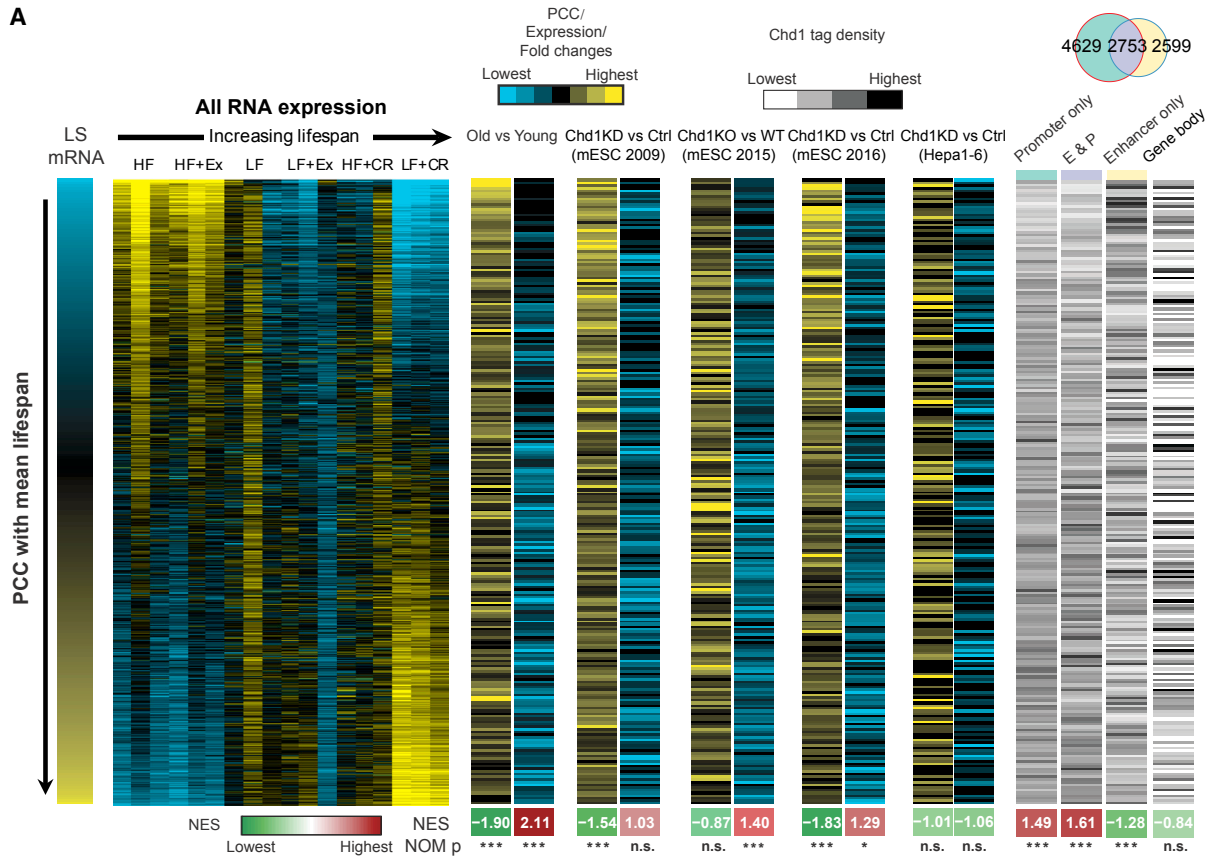

B

Up-regulated after Chd1 KD & Lifespan anti-correlated

Term	p-value
Lysosome	0.019
Natural killer cell mediated cytotoxicity	0.020
Graft-versus-host disease	0.032
Allograft rejection	0.032
NOD-like receptor signaling pathway	0.036
Type I diabetes mellitus	0.037
Autoimmune thyroid disease	0.047
Chemokine signaling pathway	0.057
Focal adhesion	0.070
Antigen processing and presentation	0.070

Down-regulated after Chd1 KD & Lifespan correlated

Term	p-value
Glycolysis / Gluconeogenesis	0.009

D

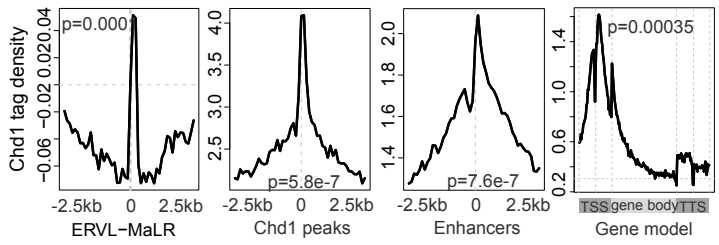

C Ranked by fold change

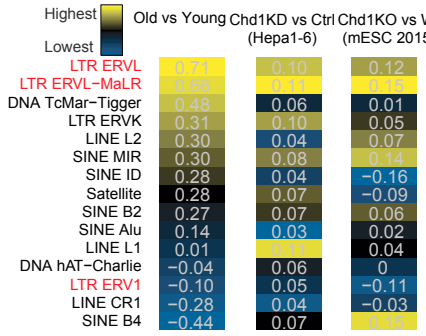

E

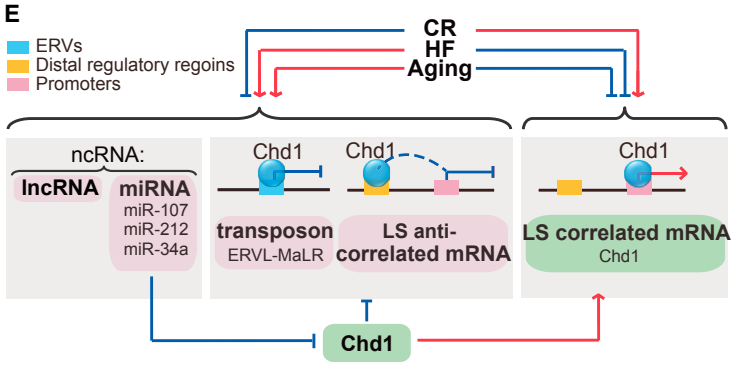

(legend on next page)

p value = 7.0e-6; for HF, p value = 0.20; and for *Chd1* KO in mESCs, p value = 0.0023 for ERVL-MaLR and ERVL against all other repeat families). We also knocked down *Chd1* in mouse hepatoma Hepa1-6 cells. Although genes differentially expressed under *Chd1* KD in Hepa1-6 cells were not enriched for LS-related genes (Figure 5A), the expressions of ERVL-MaLR and ERVL are also significantly upregulated in these cells (t test p value = 0.011 for ERVL-MaLR and ERVL against all other repeat families, Figure 5C).

Consistent with the large derepression of ERVL-MaLR by *Chd1* KD, there is a significant enrichment for Chd1 binding within the ERVL-MaLR elements compared with flanking regions (rank-sum test p = 1e-4 when comparing 300 bp downstream of the start of these transposons versus flanking ±2.5-kb regions) (Figure 5D). This suggests that Chd1 may repress transcription from these LS anti-correlated and HF-diet- and aging-activated transposon-derived repeat elements through direct binding to them (Figure 5D). Intriguingly, endogenous retroviruses (ERV) LTRs have been shown to contain binding sites for pluripotency master regulators *Oct4*, *Nanog*, *Klf4*, and *Sox2* and to be required for pluripotency of ESCs (Kunarso et al., 2010; Wang et al., 2014a). Indeed, compared to flanking sequences, these motifs are in general more enriched when these transposons are localized in the enhancer regions of LS anti-correlated and aging-activated genes than LS-correlated and aging-repressed genes, respectively (Figure S5E), consistent with there being potential enhancers for the former gene sets. Here, we defined enhancers as H3K27ac peaks that are between 50 and 2.5 kb upstream of TSS and enhancer RNAs (eRNAs) as RNAs expressed at enhancers. The RNA expression change pattern on ERVL-MaLR is similar to that of enhancer-like Chd1 peaks (H3K27ac peaks occupied by Chd1) in that they both have a peak when comparing old versus young or *Chd1* KD/KO versus control, and they both have a trough when comparing LF versus HF (Figure S5F). This suggests ERVL-MaLR might function as enhancers. Our finding of specific activation of these two types of elements by diet and aging implicates a previously unsuspected effect of diet and aging on cell stemness and pluripotency.

In contrast to the ERVL-MaLR and ERVL transcripts, *Chd1* KD does not affect the expression of other LS-correlated or anti-correlated lncRNAs (Figure S5G). This suggests that, although HF and aging globally increase ncRNA expression, the majority of the lncRNAs are not regulated through Chd1 and that its regulation of mRNA, at promoter and enhancer regions, and two types of transposon-derived repeat elements are rather specific (Figure 5E).

DISCUSSION

Here, we profiled the midlife liver transcriptome by RNA-seq and identified miRNAs, lncRNAs, and transposable elements exhibiting significant expression correlation with LS modification across six different intervention regimens. We observed three intriguing design patterns for the dietary intervention network: (1) LS-extending dietary interventions largely repressed the expression of miRNAs, lncRNAs, and transposable elements; (2) protein-coding mRNAs with expression positively correlated with long LS are highly targeted by miRNAs; and (3) miRNA-targeting interactions mainly target chromatin-related functions. *Chd1* is itself a LS positively correlated gene. Through *Chd1* KD experiments, we confirmed that diet and aging-induced global mRNA upregulation and downregulation are both recapitulated by *Chd1* KD through promoter and enhancer binding, respectively. HF diet and aging-activated, pluripotency-promoting transposon-derived repeat elements are also specifically repressed by *Chd1* (Figure 5E).

The simultaneous comparison of multiple interventions has the advantage of revealing LS-related genes and pathways at different molecular layers (coding, non-coding, and epigenetic) that could otherwise be overlooked in single intervention studies (Zhou et al., 2012). Here, pathway and network analyses identified genes with chromatin-related functions to have significant interactions with miRNAs negatively correlated with LS. Although we mainly used LS correlation as a LS-association metric in this study, the LS-correlated expressed mRNAs, lncRNAs, and miRNAs are highly significantly enriched for differentially expressed ($p < 0.05$) mRNAs, lncRNAs, and miRNAs between longest and shortest LS groups, respectively (GSEA p value <0.005 for all comparisons).

Our finding of multiple ncRNA classes displaying highly unbalanced expression profiles, largely repressed by LS-extending interventions, suggests a strong transcriptional response mediating these effects. This could occur through several possible

Figure 5. *Chd1* KD Mimics HF Diet and Aging-Induced Gene and Transposon Activation

(A) Heatmap of LS correlation (PCC) ranked genes in 50 gene bins, their expression levels, mean log2 fold change up (yellow) or down (blue) regulated when comparing old versus young and *Chd1*KD versus WT control, or their mean Chd1 binding peak tag density at promoter only, enhancer region only, both promoter and enhancer regions or gene body. Enrichment significance is shown as GSEA NES scores below the heatmap. LS, lifespan related.

(B) KEGG pathway enrichment for genes both upregulated upon *Chd1* KD and negatively correlated with LS and genes both downregulated upon *Chd1* KD and positively correlated with LS in mESC (*Chd1*KD mESC 2016).

(C) Fold change (log2 transformed) of repeats in old versus young mice, *Chd1* KD versus control (Ctrl) Hepa1-6 and *Chd1* KO versus WT mESCs. Repeats in red font are significantly related with LS extension (Figure 1E) or aging (Figure S3C). See Figure S5D for *Chd1* expression changes.

(D) Profile of Chd1 normalized average tag density (log2 fold change relative to input) on ERVL-MaLR, Chd1 peaks, and enhancers together with their flanking regions (upstream and downstream 2.5 kb) or at TSS, transcription termination site (TTS), and gene body. Enhancers are defined as H3K27ac peaks that are between 50 and 2.5 kb upstream of TSS. Enrichment p value is calculated by comparing 300 bp from the start of a repeat/enhancer or 500 bp upstream and downstream of TSS to their flanking 2.5 kb using the rank-sum test.

(E) A model for the opposing regulatory effects of LS-extending interventions and aging on ncRNA expression, transposon elements, and mRNA. Within ncRNAs, many miRNAs repress chromatin modification genes, in particular, three such miRNAs repress Chd1, which further regulates LS and aging-related genes in two opposite ways, represses transposons (potentially as enhancers) and LS anti-correlated genes by enhancer binding and activates LS positively correlated genes by promoter binding. LS, lifespan. See also Figure S5.

mechanisms, including inflammatory and metabolic regulation through specific transcription factors. Indeed, motif analysis revealed that the miRNAs and lncRNAs anti-correlated with LS are enriched for TFs that are associated with inflammation (e.g., *Atf4*, *Tcf12*, *Rela*), metabolic regulation (e.g., *Ppara*, *Pparg*), and hypoxia (*Hif1a*, *Hif2a*) (Figures S6A–S6C). In addition, genes associated with inflammation are highly enriched in our LS negatively correlated mRNAs, and metabolic functions are enriched in mRNAs both negatively and positively correlated with LS (Table S2; Zhou et al., 2012). Examination of components mediating insulin resistance demonstrated inflammatory cytokines and saturated fatty acids modulate miRNA expression, such as induction of miR-34a, through activation of *NF-kappa B* and *p53* (Lovis et al., 2008; Roggli et al., 2010). In contrast to HF diet, CR reduces inflammatory signaling and expression of related genes below normal levels in part through hormonal regulation (Omodei and Fontana, 2011). Similarly, CR-mediated repression is evident for multiple ncRNA classes shown here and in reports of CR in prevention or reversal of miRNA expression changes that occur during aging, a process associated with a gradual increase in inflammation (Figure 1, Khanna et al., 2011; Mercken et al., 2013; Mori et al., 2012; Olivo-Marston et al., 2014).

Using a bipartite network analysis approach, we identified miR-34a, miR-107, and miR-212-3p to target multiple genes with functions associated with chromatin, particularly the remodeler *Chd1*. *Chd1* is part of one of four chromatin remodeling ATPase families (Petty and Pillus, 2013). Functional studies found *Chd1* activity represses cryptic intragenic transcription in yeast; however, it is also required for preserving euchromatin states in embryonic stem cells and for efficient somatic cell reprogramming (Gaspar-Maia et al., 2009; Smolle et al., 2012). Additionally, it is necessary for RNA polymerase II to overcome the nucleosome barrier during transcription initiation and for nucleosome reassembly following transcription elongation (Petty and Pillus, 2013; Skene et al., 2014). Thus, *Chd1* is required for both transcription activation and cryptic transcription repression. Our finding that LS correlated and anti-correlated genes are activated and repressed by Chd1 through promoter and enhancer binding, respectively, reconciles the two contradictory functions reported for *Chd1* and provides a molecular mechanism for the two opposing modes of regulation. That is, depending on different genomic contexts and binding partners, *Chd1* can either open or close local chromatin to activate or repress transcription.

Deletion of *Chd1* in yeast has been reported to extend replicative and reduce chronological LS (Dang et al., 2014; Laschober et al., 2010). Nevertheless, our results point to a role for miRNA control of *Chd1* and other chromatin-related genes in mediating the effects of LS-modulating dietary interventions. Specifically, we demonstrate that KD of *Chd1*, which is repressed by HF diet and in old mice, mimics mRNA changes and transposon derepression associated with reduced LS and aging. Of particular interest, these repeat elements are known to regulate pluripotency and here are found to be specifically repressed by *Chd1*, upregulated by aging and associated with reduced LS. These provide a potentially missing molecular link between aging/LS and cell pluripotency.

How dietary interventions integrate multiple levels of transcriptional regulation to affect longevity is an area of active investigation. Here, we provide a map of the global ncRNA changes and network design principles associated with LS modification and aging. Mechanistically, we also identified LS-related miRNA-target gene interactions involved in regulating genes critical for maintaining chromatin stability. Together, miRNAs targeting of chromatin remodelers, such as *Chd1* to mediate dietary-intervention-induced mRNA expression and transposon suppression, is a mode of crosstalk among miRNAs, chromatin remodelers, and transposons.

EXPERIMENTAL PROCEDURES

Tissue Preparation

The Institutional Animal Care and Use Committee of the Institute for Nutritional Sciences, Chinese Academy of Sciences, approved all animal procedures and protocols used in this study. Midlife (62 weeks of age) male C57BL/6J mice liver samples, individual-matched liver/serum physiological measurements, and group mean/maximum LS were obtained from a previous study (Zhou et al., 2012). Frozen liver tissues (n = 3 per group) from one of six intervention groups beginning at 5 weeks of age (ad libitum feeding of LF diet [10% fat] or HF diet [60% fat], LF or HF diet with access to voluntary Ex, and LF or HF diet calorie restricted by 30%) were directly homogenized in Trizol (Life Technologies) and subsequently used to isolate total RNA, which are then subjected to standard poly(A)+ RNA-seq (Supplemental Experimental Procedures).

RNA-Seq and Microarray Processing and Analysis

The raw 100-bp single-end reads from RNA-seq, from both dietary intervention in mouse liver, *Chd1* KD in Hepa1-6 cells, were uniquely mapped to UCSC mm10 genome with TopHat (v.1.4.1, -N 3) and guided by UCSC mm10 RefGene annotation (downloaded on February 23, 2013). The mapped reads were then summarized to RPKM (reads per kilobases per million mapped) for RefSeq genes with Cufflinks (v.1.3.0). Lowly expressed genes were filtered out by RPKM $\geq$1 in at least three dietary intervention samples for miRNAs, mRNA, and known lncRNAs and at least two Hepa1-6 cell samples. The retained genes were log-transformed for downstream analysis. Known lncRNAs refer to the annotated ncRNAs longer than 200 bp.

lncRNAs were inferred similar to Cabili et al. (2011) as follows: (1) spliced transcript determination: reads were aligned twice to mm10 with TopHat, first to infer junctions for each sample and then pooled to guide the second alignment; (2) transcript length >200 bp; (3) transcript identification: transcripts were compared to RefSeq mm10 transcripts (Cuffcompare v.1.3.0) with class code "." or "u," and no ReferenceID; (4) non-coding transcripts: coding potential (CPAT v.1.2.1) <0.44 (the optimum mouse coding probability used by this software); (5) additionally, we filtered for high-confidence lncRNAs, with RPKM $\geq$1 in at least 9 out of the 18 samples.

Small RNA-Seq Processing and Analysis

Small RNA-seq reads were trimmed for 3′ and 5′ adaptor sequences, and only trimmed sequences 18–31 bp were exactly mapped to the mm10 genome with SOAP2 (version 2.20). Mature miRNAs were annotated with mirBase version 19, quantified similar to Hu et al. (2011) and normalized to reads per million isomiR reads (RPMs). Lowly expressed miRNAs were filtered out by RPM $\geq$1 in at least three samples. The retained miRNAs were log-transformed for downstream analysis.Transposable Element/Repeat Mapping.

To quantify transcription from specific repeat loci, the coverage of TopHat-mapped data on repeat loci of UCSC mm10 genome (http://genome.ucsc.edu/cgibin/hgTables?hgsid=582025637_ZFwzdrOL0m4QQqRYhuoL1d1Va043&clade=mammal&org=Mouse&db=mm10&hgta_group=allTables&hgta_track=mm10&hgta_table=rmsk&hgta_regionType=genome&position=chr12%3A56694976-56714605&hgta_outputType=primaryTable&hgta_outFileName=, downloaded on March 21, 2014) was summarized with featureCounts (v.1.4.6-p1) and normalized as RPKM (Liao et al., 2014). To quantify transcription from specific repeat families, the sequences of each repeat family were

retrieved, extended with flanking region (to guarantee over 50% in mapping), and then built as reference. The reads were considered as transcripts from a repeat family if they mapped to corresponding reference with SOAPaligner (v.2.20) (Li et al., 2009). To compare across samples, the mapped read count of each repeat family was normalized by the total mapped read count to the UCSC mm10 genome reference. Transposable elements (TEs) are repeats of class DNA, long interspersed elements (LINE), short interspersed elements (SINE), and LTR.

miRNA Target Gene Enrichment

The potential regulating pairs were filtered by various criteria: (1) all TargetScan pairs; (2) TargetScan pairs with miRNA expressed in this study; (3) TargetScan pairs with expression PCC <0 between miRNA and mRNA; (4) TargetScan pairs with PCC < -0.46 ($p < 0.05$); (5) TargetScan pairs with PCC < -0.58 ($p < 0.01$); and (6) TargetScan pairs with PCC < -0.7 ($p < 0.001$). For each criterion, the enrichment of miRNA regulation was examined for each miRNA or all miRNAs that pass the filter. For an individual miRNA's target gene set, the positively or negatively LS-related mRNA set was regarded as significantly regulated by a miRNA if the Fisher's exact test had a $p < 0.05$ for target enrichment. Then, the significance of the number of miRNAs whose targets are significantly enriched was further determined by 1,000 time permutations. The fold ratio was estimated by observation over background expectation (average). For pooled mRNA targets, all regulating pairs were pooled into one regulating set. The significance of its overlap with the LS-related mRNA sets was determined by Fisher's exact test (with Bonferroni correction). The fold ratio was estimated by observation over background expectation.

Bipartite Network Construction

The bipartite network was constructed based on the following criteria: (1) all nodes (mRNAs, miRNAs) in the network were significantly associated with LS (PCC $p < 0.001$, an approximate $|PCC| > 0.7$); (2) all miRNAs are broadly conserved among vertebrates; (3) all edges represent miRNA-mRNA TargetScan pairs with a miRNA to mRNA expression negative PCC $p < 0.05$ (corresponding to PCC < -0.46). The layout of network was illustrated with Cytoscape (version 2.8.3).

ACCESSION NUMBERS

The accession number for the sequencing data reported in this paper is GEO: GSE87514.

SUPPLEMENTAL INFORMATION

Supplemental Information includes Supplemental Experimental Procedures, six figures, and six tables and can be found with this article online at http://dx.doi.org/10.1016/j.celrep.2017.03.001.

AUTHOR CONTRIBUTIONS

J.-D.J.H. and C.D.G. conceived the study. J.-D.J.H., C.D.G., and Y.H. designed analyses and experiments with suggestions from others. Y.H. and X.D. conducted computational analyses. C.D.G. performed wet lab experiments. Liver samples were collected by L.Y. under the direction of Y.L. J.-D.J.H., C.D.G., Y.H., and X.D. analyzed the data and wrote the manuscript.

ACKNOWLEDGMENTS

This work was supported by grants from China Ministry of Science and Technology 2015CB964803 and 2016YFE0108700, National Natural Science Foundation of China 91329302, 31210103916, and 91519330, and Chinese Academy of Sciences XDB19020301 and XDA01010303 to J.-D.J.H. and by the Chinese Academy of Sciences Fellowship for Young International Scientists 2010Y2SB06, SIBS Postdoctoral Research Grant 2013KIP315, and the National Natural Science Foundation of China 31350110327 and 31250110212 to C.D.G.

Received: October 4, 2016
Revised: January 17, 2017
Accepted: February 28, 2017
Published: March 21, 2017

REFERENCES

Bartel, D.P. (2004). MicroRNAs: Genomics, biogenesis, mechanism, and function. Cell *116*, 281–297.

Bochkis, I.M., Przybylski, D., Chen, J., and Regev, A. (2014). Changes in nucleosome occupancy associated with metabolic alterations in aged mammalian liver. Cell Rep. *9*, 996–1006.

Boehm, M., and Slack, F. (2005). A developmental timing microRNA and its target regulate life span in C. elegans. Science *310*, 1954–1957.

Boon, R.A., Iekushi, K., Lechner, S., Seeger, T., Fischer, A., Heydt, S., Kaluza, D., Tréguer, K., Carmona, G., Bonauer, A., et al. (2013). MicroRNA-34a regulates cardiac ageing and function. Nature *495*, 107–110.

Cabili, M.N., Trapnell, C., Goff, L., Koziol, M., Tazon-Vega, B., Regev, A., and Rinn, J.L. (2011). Integrative annotation of human large intergenic noncoding RNAs reveals global properties and specific subclasses. Genes Dev. *25*, 1915–1927.

Carrer, M., Liu, N., Grueter, C.E., Williams, A.H., Frisard, M.I., Hulver, M.W., Bassel-Duby, R., and Olson, E.N. (2012). Control of mitochondrial metabolism and systemic energy homeostasis by microRNAs 378 and 378*. Proc. Natl. Acad. Sci. USA *109*, 15330–15335.

Choi, S.E., and Kemper, J.K. (2013). Regulation of SIRT1 by microRNAs. Mol. Cells *36*, 385–392.

Choi, S.E., Fu, T., Seok, S., Kim, D.H., Yu, E., Lee, K.W., Kang, Y., Li, X., Kemper, B., and Kemper, J.K. (2013). Elevated microRNA-34a in obesity reduces NAD+ levels and SIRT1 activity by directly targeting NAMPT. Aging Cell *12*, 1062–1072.

Christoffersen, N.R., Shalgi, R., Frankel, L.B., Leucci, E., Lees, M., Klausen, M., Pilpel, Y., Nielsen, F.C., Oren, M., and Lund, A.H. (2010). p53-independent upregulation of miR-34a during oncogene-induced senescence represses MYC. Cell Death Differ. *17*, 236–245.

Dang, W., Sutphin, G.L., Dorsey, J.A., Otte, G.L., Cao, K., Perry, R.M., Wanat, J.J., Saviolaki, D., Murakami, C.J., Tsuchiyama, S., et al. (2014). Inactivation of yeast Isw2 chromatin remodeling enzyme mimics longevity effect of calorie restriction via induction of genotoxic stress response. Cell Metab. *19*, 952–966.

de Dieuleveult, M., Yen, K., Hmitou, I., Depaux, A., Boussouar, F., Bou Dargham, D., Jounier, S., Humbertclaude, H., Ribierre, F., Baulard, C., et al. (2016). Genome-wide nucleosome specificity and function of chromatin remodellers in ES cells. Nature *530*, 113–116.

de Lencastre, A., Pincus, Z., Zhou, K., Kato, M., Lee, S.S., and Slack, F.J. (2010). MicroRNAs both promote and antagonize longevity in C. elegans. Curr. Biol. *20*, 2159–2168.

de Magalhães, J.P., Costa, J., and Toussaint, O. (2005). HAGR: The Human Ageing Genomic Resources. Nucleic Acids Res. *33*, D537–D543.

Flanagan, J.F., Mi, L.Z., Chruszcz, M., Cymborowski, M., Clines, K.L., Kim, Y., Minor, W., Rastinejad, F., and Khorasanizadeh, S. (2005). Double chromodomains cooperate to recognize the methylated histone H3 tail. Nature *438*, 1181–1185.

Fontana, L., Partridge, L., and Longo, V.D. (2010). Extending healthy life span–from yeast to humans. Science *328*, 321–326.

Gaspar-Maia, A., Alajem, A., Polesso, F., Sridharan, R., Mason, M.J., Heidersbach, A., Ramalho-Santos, J., McManus, M.T., Plath, K., Meshorer, E., and Ramalho-Santos, M. (2009). Chd1 regulates open chromatin and pluripotency of embryonic stem cells. Nature *460*, 863–868.

Guzman-Ayala, M., Sachs, M., Koh, F.M., Onodera, C., Bulut-Karslioglu, A., Lin, C.J., Wong, P., Nitta, R., Song, J.S., and Ramalho-Santos, M. (2015). Chd1 is essential for the high transcriptional output and rapid growth of the mouse epiblast. Development *142*, 118–127.

He, L., He, X., Lim, L.P., de Stanchina, E., Xuan, Z., Liang, Y., Xue, W., Zender, L., Magnus, J., Ridzon, D., et al. (2007). A microRNA component of the p53 tumour suppressor network. Nature *447*, 1130–1134.

Hu, H.Y., Guo, S., Xi, J., Yan, Z., Fu, N., Zhang, X., Menzel, C., Liang, H., Yang, H., Zhao, M., et al. (2011). MicroRNA expression and regulation in human, chimpanzee, and macaque brains. PLoS Genet. *7*, e1002327.

Kato, M., and Slack, F.J. (2013). Ageing and the small, non-coding RNA world. Ageing Res. Rev. *12*, 429–435.

Khanna, A., Muthusamy, S., Liang, R., Sarojini, H., and Wang, E. (2011). Gain of survival signaling by down-regulation of three key miRNAs in brain of calorie-restricted mice. Aging (Albany NY) *3*, 223–236.

Kunarso, G., Chia, N.Y., Jeyakani, J., Hwang, C., Lu, X., Chan, Y.S., Ng, H.H., and Bourque, G. (2010). Transposable elements have rewired the core regulatory network of human embryonic stem cells. Nat. Genet. *42*, 631–634.

Laschober, G.T., Ruli, D., Hofer, E., Muck, C., Carmona-Gutierrez, D., Ring, J., Hutter, E., Ruckenstuhl, C., Micutkova, L., Brunauer, R., et al. (2010). Identification of evolutionarily conserved genetic regulators of cellular aging. Aging Cell *9*, 1084–1097.

Lewis, B.P., Burge, C.B., and Bartel, D.P. (2005). Conserved seed pairing, often flanked by adenosines, indicates that thousands of human genes are microRNA targets. Cell *120*, 15–20.

Li, R., Yu, C., Li, Y., Lam, T.W., Yiu, S.M., Kristiansen, K., and Wang, J. (2009). SOAP2: An improved ultrafast tool for short read alignment. Bioinformatics *25*, 1966–1967.

Li, N., Muthusamy, S., Liang, R., Sarojini, H., and Wang, E. (2011). Increased expression of miR-34a and miR-93 in rat liver during aging, and their impact on the expression of Mgst1 and Sirt1. Mech. Ageing Dev. *132*, 75–85.

Liao, Y., Smyth, G.K., and Shi, W. (2014). featureCounts: An efficient general purpose program for assigning sequence reads to genomic features. Bioinformatics *30*, 923–930.

Liu, N., Landreh, M., Cao, K., Abe, M., Hendriks, G.J., Kennerdell, J.R., Zhu, Y., Wang, L.S., and Bonini, N.M. (2012). The microRNA miR-34 modulates ageing and neurodegeneration in Drosophila. Nature *482*, 519–523.

Lovis, P., Roggli, E., Laybutt, D.R., Gattesco, S., Yang, J.Y., Widmann, C., Abderrahmani, A., and Regazzi, R. (2008). Alterations in microRNA expression contribute to fatty acid-induced pancreatic beta-cell dysfunction. Diabetes *57*, 2728–2736.

Maes, O.C., An, J., Sarojini, H., and Wang, E. (2008). Murine microRNAs implicated in liver functions and aging process. Mech. Ageing Dev. *129*, 534–541.

Mercken, E.M., Carboneau, B.A., Krzysik-Walker, S.M., and de Cabo, R. (2012). Of mice and men: The benefits of caloric restriction, exercise, and mimetics. Ageing Res. Rev. *11*, 390–398.

Mercken, E.M., Majounie, E., Ding, J., Guo, R., Kim, J., Bernier, M., Mattison, J., Cookson, M.R., Gorospe, M., de Cabo, R., and Abdelmohsen, K. (2013). Age-associated miRNA alterations in skeletal muscle from rhesus monkeys reversed by caloric restriction. Aging (Albany NY) *5*, 692–703.

Mori, M.A., Raghavan, P., Thomou, T., Boucher, J., Robida-Stubbs, S., Macotela, Y., Russell, S.J., Kirkland, J.L., Blackwell, T.K., and Kahn, C.R. (2012). Role of microRNA processing in adipose tissue in stress defense and longevity. Cell Metab. *16*, 336–347.

Nakanishi, N., Nakagawa, Y., Tokushige, N., Aoki, N., Matsuzaka, T., Ishii, K., Yahagi, N., Kobayashi, K., Yatoh, S., Takahashi, A., et al. (2009). The up-regulation of microRNA-335 is associated with lipid metabolism in liver and white adipose tissue of genetically obese mice. Biochem. Biophys. Res. Commun. *385*, 492–496.

Olivo-Marston, S.E., Hursting, S.D., Perkins, S.N., Schetter, A., Khan, M., Croce, C., Harris, C.C., and Lavigne, J. (2014). Effects of calorie restriction and diet-induced obesity on murine colon carcinogenesis, growth and inflammatory factors, and microRNA expression. PLoS ONE *9*, e94765.

Omodei, D., and Fontana, L. (2011). Calorie restriction and prevention of age-associated chronic disease. FEBS Lett. *585*, 1537–1542.

Petty, E., and Pillus, L. (2013). Balancing chromatin remodeling and histone modifications in transcription. Trends Genet. *29*, 621–629.

Roggli, E., Britan, A., Gattesco, S., Lin-Marq, N., Abderrahmani, A., Meda, P., and Regazzi, R. (2010). Involvement of microRNAs in the cytotoxic effects exerted by proinflammatory cytokines on pancreatic beta-cells. Diabetes *59*, 978–986.

Sandberg, R., Neilson, J.R., Sarma, A., Sharp, P.A., and Burge, C.B. (2008). Proliferating cells express mRNAs with shortened 3′ untranslated regions and fewer microRNA target sites. Science *320*, 1643–1647.

Sims, R.J., 3rd, Chen, C.F., Santos-Rosa, H., Kouzarides, T., Patel, S.S., and Reinberg, D. (2005). Human but not yeast CHD1 binds directly and selectively to histone H3 methylated at lysine 4 via its tandem chromodomains. J. Biol. Chem. *280*, 41789–41792.

Skene, P.J., Hernandez, A.E., Groudine, M., and Henikoff, S. (2014). The nucleosomal barrier to promoter escape by RNA polymerase II is overcome by the chromatin remodeler Chd1. eLife *3*, e02042.

Smith-Vikos, T., de Lencastre, A., Inukai, S., Shlomchik, M., Holtrup, B., and Slack, F.J. (2014). MicroRNAs mediate dietary-restriction-induced longevity through PHA-4/FOXA and SKN-1/Nrf transcription factors. Curr. Biol. *24*, 2238–2246.

Smolle, M., Venkatesh, S., Gogol, M.M., Li, H., Zhang, Y., Florens, L., Washburn, M.P., and Workman, J.L. (2012). Chromatin remodelers Isw1 and Chd1 maintain chromatin structure during transcription by preventing histone exchange. Nat. Struct. Mol. Biol. *19*, 884–892.

Solon-Biet, S.M., McMahon, A.C., Ballard, J.W., Ruohonen, K., Wu, L.E., Cogger, V.C., Warren, A., Huang, X., Pichaud, N., Melvin, R.G., et al. (2014). The ratio of macronutrients, not caloric intake, dictates cardiometabolic health, aging, and longevity in ad libitum-fed mice. Cell Metab. *19*, 418–430.

Tam, S., Tsao, M.S., and McPherson, J.D. (2015). Optimization of miRNA-seq data preprocessing. Brief. Bioinform. *16*, 950–963.

Trajkovski, M., Hausser, J., Soutschek, J., Bhat, B., Akin, A., Zavolan, M., Heim, M.H., and Stoffel, M. (2011). MicroRNAs 103 and 107 regulate insulin sensitivity. Nature *474*, 649–653.

Vickers, K.C., Shoucri, B.M., Levin, M.G., Wu, H., Pearson, D.S., Osei-Hwedieh, D., Collins, F.S., Remaley, A.T., and Sethupathy, P. (2013). MicroRNA-27b is a regulatory hub in lipid metabolism and is altered in dyslipidemia. Hepatology *57*, 533–542.

Vora, M., Shah, M., Ostafi, S., Onken, B., Xue, J., Ni, J.Z., Gu, S., and Driscoll, M. (2013). Deletion of microRNA-80 activates dietary restriction to extend C. elegans healthspan and lifespan. PLoS Genet. *9*, e1003737.

Wang, J., Xie, G., Singh, M., Ghanbarian, A.T., Raskó, T., Szvetnik, A., Cai, H., Besser, D., Prigione, A., Fuchs, N.V., et al. (2014a). Primate-specific endogenous retrovirus-driven transcription defines naive-like stem cells. Nature *516*, 405–409.

Wang, N., Liu, J., Xie, F., Gao, X., Ye, J.H., Sun, L.Y., Wei, R., Yang, B.F., and Ai, J. (2014b). miR-124/ATF-6, a novel lifespan extension pathway of astragalus polysaccharide in C. elegans. J. Cell. Biochem. *116*, 242–251.

Xu, P., Vernooy, S.Y., Guo, M., and Hay, B.A. (2003). The Drosophila microRNA Mir-14 suppresses cell death and is required for normal fat metabolism. Curr. Biol. *13*, 790–795.

Zhou, B., Yang, L., Li, S., Huang, J., Chen, H., Hou, L., Wang, J., Green, C.D., Yan, Z., Huang, X., et al. (2012). Midlife gene expressions identify modulators of aging through dietary interventions. Proc. Natl. Acad. Sci. USA *109*, E1201–E1209.